Chapter 2

Novel combination of collagen dynamics analysis and transcriptional profiling reveals fibrosis-relevant genes and pathways

Matrix Biology, 2013

Marjolein E. Blaauboer
Claire L. Emson, Lars Verschuren, Marjan van Erk, Scott M. Turner, Vincent Everts, Roeland Hanemaaijer, Reinout Stoop

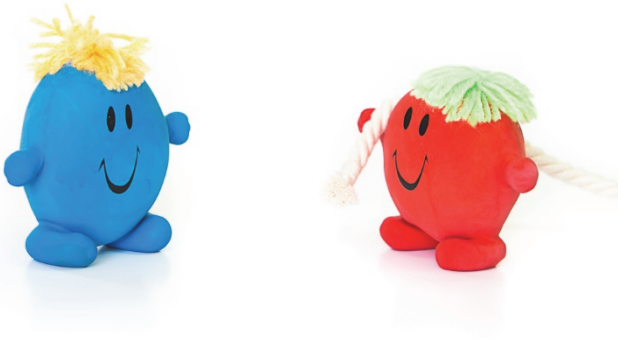

Abstract

Collagen deposition is a key process during idiopathic pulmonary fibrosis; however, little is known about the dynamics of collagen formation during disease development. Tissue samples of early stages of human disease are not readily available and it is difficult to identify changes in collagen content, since standard collagen analyses do not distinguish between 'old' and 'new' collagen. Therefore, the current study aimed to (i) investigate the dynamics of new collagen formation in mice using bleomycin-induced lung fibrosis in which newly synthesized collagen was labelled with deuterated water and (ii) use this information to identify genes and processes correlated with new collagen formation.

Lung fibrosis was induced in female C57Bl/6 mice by bleomycin instillation. Animals were sacrificed at 1 to 5 weeks after fibrosis induction. Collagen synthesized during the week before sacrifice was labelled with deuterium by providing mice with deuterated drinking water. After sacrifice, we collected lung tissue for microarray analysis, determination of new collagen formation, and histology. Furthermore, we measured *in vitro* the expression of selected genes after transforming growth factor (TGF)β_1-induced myofibroblast differentiation.

Deuterated water labelling showed a strong increase in new collagen formation already during the first week after fibrosis induction and a complete return to baseline at five weeks. Correlation of new collagen formation data with gene expression data allowed us to create a gene expression signature of fibrosis within the lung and revealed fibrosis-specific processes, amongst which proliferation. This was confirmed by measuring cell proliferation and collagen synthesis simultaneously using deuterated water incorporation in a separate experiment. Furthermore, new collagen formation strongly correlated with gene expression of e.g. elastin, Wnt-1 inducible signalling pathway protein 1, tenascin C, lysyl oxidase, and type V collagen. Gene expression of these genes was upregulated *in vitro* in fibroblasts stimulated with TGFβ_1.

Together, these data demonstrate, using a novel combination of technologies, that the core process of fibrosis, i.e. the formation of new collagen, correlates not only with a wide range of genes involved in general extracellular matrix production and modification but also with cell proliferation. The observation that the large majority of the genes which correlated with new collagen formation also were upregulated during TGFβ_1-induced myofibroblast differentiation provides further evidence for their involvement in fibrosis.

Introduction

Idiopathic pulmonary fibrosis (IPF) is a devastating fibrosing lung disease and is characterized by excessive matrix deposition, destroying both tissue architecture and function. The incidence of IPF is estimated to be 5 to 10 in 100,000 (Fernandez Perez et al., 2010); most patients die within 2 to 5 years after diagnosis. This is related to the fact that IPF is often diagnosed quite late, due to the overcapacity of the lung tissue. Only once extensive damage to the lung tissue has taken place, symptoms such as shortness of breath occur leading to diagnosis. Because of this late diagnosis, the aetiology of IPF is largely unknown and little information is available about the early phases in the development of lung fibrosis. To gain more insight into these early phases of fibrosis development, research heavily relies on animal models (Chua et al., 2005).

The most extensively used model to study lung fibrosis uses intratracheal instillation of bleomycin into the lungs of mice as an inducer (Chua et al., 2005; Moeller et al., 2008). The proposed mechanism is that bleomycin-induced generation of reactive oxygen species results in extensive epithelial necropsy. This damage induces an inflammatory response with a peak around one week after bleomycin instillation, followed by a phase in which extensive fibrotic remodelling occurs (Chaudhary et al., 2006; Moeller et al., 2008). To elucidate which genes and processes are involved in the development of fibrosis, microarray analyses have been used (Hannivoort et al., 2012; Kaminski et al., 2000). These type of studies have shown that during the development of bleomycin-induced lung fibrosis, many changes in gene expression patterns occur. However, as with all animal models, it is difficult to distinguish which processes are important for fibrosis development in general and which represent model-specific changes. Therefore, the challenge is how to identify the fibrosis-specific pathways from the total changes in gene expression.

Collagen deposition is the hallmark of fibrosis. In the bleomycin model total collagen content of the lung, measured by the amount of hydroxyproline (Hyp), is a standard outcome parameter used to evaluate fibrosis (Chua et al., 2005). However, this parameter is sometimes less than optimal since healthy lung already contains substantial amounts of collagen, making it difficult to identify subtle but important changes in collagen deposition early in the process of fibrosis. Therefore, in the current study we focused on the formation of newly synthesized collagen during the 7 days prior to sacrifice by deuterated water labelling. The deuterated water is incorporated into all proteins produced during this period and after sacrifice the amount of labelled hydroxyproline is a parameter of newly deposited collagen (Gardner et al., 2007).

Many processes have been described to be upregulated during experimental lung fibrosis, such as activation of macrophages and neutrophils (Moeller et al., 2008), inflammatory cytokine production (Moeller et al., 2008), transforming growth factor (TGF)β-signalling (Degryse et al., 2011), and epithelial-to-mesenchymal transition (Tanjore

et al., 2009). The contribution of these processes is to the fibrotic process occurring in the lung is still unclear. Therefore, we aimed in this study to identify which genes and processes specifically relate to the collagen deposition during bleomycin-induced lung fibrosis by combining new collagen formation with gene expression data at different time points after bleomycin treatment. Our results indicate a strong correlation of new collagen formation with processes such as cell proliferation and extracellular matrix production and with specific genes. We provided further evidence for involvement of these genes in lung fibrosis by showing increased expression after TGFβ_1-induced myofibroblast differentiation *in vitro*. This provides new leads towards the understanding of the aetiology of lung fibrosis.

Experimental Procedures

Animal procedures

All animal procedures were approved by TNO Animal Welfare Committee (#2738). Female C57Bl/6J mice (Charles River Laboratories, Germany) 10 to 12 weeks of age received intratracheal instillation of 30 µl bleomycin (Pharmachemie BV, Haarlem, The Netherlands; 1.25 U/ml in PBS). To label new collagen, at 7 days before sacrifice, the mice received 35 µl deuterated water (D_2O) / gram body weight (i.p.) and normal drinking water was replaced with 8% deuterated water designed to result in a final body water enrichment of approximately 5% deuterium in the animal. This low percentage of deuterated water was used to prevent any interacting effects of the deuterated water on the bleomycin-induced lung fibrosis, as observed by Gaeng and colleagues (Gaeng et al., 1995). Water was refreshed every second day.

Mice were sacrificed by CO_2 asphyxiation at 1 (n=8), 2 (n=8), 3 (n=8), 4 (n=6) or 5 (n=7) weeks after bleomycin treatment. Untreated animals were used as control (t = 0 wk, n=7). After sacrifice, the left lung lobe was fixed with 10% formalin and processed for histology; the cranial lung lobe was stored at -80°C until determination of D_2O incorporation in Hyp while the caudal lobe was snap-frozen in liquid nitrogen for microarray analysis.

In a separate set of experiments, mice were sacrificed at 2 weeks after intratracheal instillation of bleomycin (Sigma Aldrich, St. Louis, MO, USA; 1.5 U/kg) (n=13 and 15) or saline (n=4 and 5). Data represent two experiments. These mice received deuterated water during the 14 days before sacrifice. Lung tissue was snap frozen and analysed for cell proliferation and collagen deposition determination by deuterated water labelling.

Histology

Formalin-fixed tissues were embedded in paraffin, sectioned in 5 µm sections, and stained with Masson's Trichrome staining. Severity of fibrosis was determined using a modified Ashcroft score (Hübner et al., 2008).

Kinetic analysis

Deuterated water incorporation into hydroxyproline and DNA were analysed as described earlier (Gardner et al., 2007; Neese et al., 2002, 2001; Varady et al., 2007).

For hydroxyproline kinetic analysis, tissue was homogenized in normal abundance water and the homogenate was subjected to two rounds of acetone precipitation at -20°C to obtain the total tissue protein for Hyp assessment. The proteins were hydrolyzed using HCl, dried under vacuum and suspended in a solution of 50% acetonitrile, 50 mM K_2HPO_4 and pentafluorobenzyl bromide before incubation. Derivatives were extracted by ethyl acetate, and the top layer was removed and dried by vacuum centrifugation. In order to acetylate the hydroxyl moiety of Hyp, samples were incubated with a solution of

acetonitrile, N-Methyl-N[tert-butyldimethyl-dilyl]trifluoroacetamide and methylimidizole. This material was extracted in petroleum ether and dried with Na_2SO_4. The derivatized Hyp was analysed by gas chromatography-mass spectrometry (GC-MS), performed in the negative chemical ionization mode. Selected ion monitoring was performed on ions with mass-to-charge ratios (m/z) 425 and 426, which include all of the carbon-hydrogen bonds from Hyp.

For cell proliferation kinetics, DNA was isolated from lung tissue using the DNeasy kit (Qiagen, Valencia, CA). Purified DNA was hydrolyzed to free deoxyribonucleosides and the deoxyribose moiety of purine deoxyribonucleosides derivatized to pentane tetra-acetate for analysis by GC-MS, as described elsewhere (Neese et al., 2002, 2001; Varady et al., 2007).

^2H_2O enrichment in plasma was determined using a previously described method (Previs et al., 1996). Briefly, body water was evaporated from plasma by overnight incubation at 80˚C. Samples were then mixed in 10M NaOH and acetone followed by a second overnight incubation. This material was extracted in hexane and dried with Na_2SO_4 prior to GC-MS analysis.Gas chromatography was performed utilizing a DB-17 GC column. Mass spectrometry was performed in NCI mode with helium as the carrier gas, and m/z ratios 435-436, corresponding to the M0 and M1 mass isotopomers of pentane tetra-acetate, were analyzed by SIM.

Incorporation of ^2H into Hyp or DNA was calculated as the molar fraction of molecules with one excess mass unit above the natural abundance fraction (EM1). Fractional turnover was calculated as the ratio of the measured EM1 to the asymptotic value of EM1, representing the maximal EM1 in a population of fully turned-over cells or proteins possible at the water enrichment present.

Microarray analysis

Total RNA was isolated by homogenization of lung specimens in Trizol, followed by a DNAse treatment (Qiagen, Hilden, Germany) and use of the RNeasy Mini Kit for RNA extraction (Qiagen). RNA quality control was performed with Agilent Bioanalyser (Agilent Technologies, Santa Clara, CA, USA). The Illumina TotalPrep RNA Amplification Kit (Ambion, Huntington, UK) was used to synthesize biotin labeled cRNA starting with 500 ng total RNA. Aliquots of each sample were hybridized to an Illumina MouseRef-8 V2 expression bead-chip (Illumina Inc., San Diego CA, USA).

Gene expression data were extracted using BeadStudio. Background subtracted data were submitted to quantile normalization in GeneSpring and were log2 transformed. Next a filter was applied to remove genes that were not detected (retaining genes with p value > 0.99 in at least 4 samples), resulting in a filtered set of 13481 probes for further analysis. All remaining values below 2.32 (5 on non-log scale) were floored to 2.32. Gene expression

changes were calculated as 2log ratios compared to mean expression in control mice (t = 0 week).

Gene expression data were analyzed by Tox-profiler software version December 2009 (Boorsma et al., 2005), a tool that uses the *t*-test to score changes in the average activity of predefined groups of genes. The gene groups are defined based on GO categorization. MetaCore version 6.9 (GeneGo/Thomson Reuters, USA; http://www.genego.com/metacore.php) was used for pathway analysis.

The data discussed in this chapter have been deposited in NCBI's Gene Expression Omnibus (Edgar et al., 2002) and are accessible through GEO Series accession number GSE37635 (http://www.ncbi.nlm.nih.gov/geo/query/acc.cgi?acc=GSE37635).

Table 1: Gene product, Gene, GenBank ID, and Assay-on-Demand™ used in this study.

Gene product	Gene	GenBank ID	Assay-on-Demand™
α-smooth muscle actin	ACTA2	NM_001613.2	Hs00426835_g1
α_1 chain type I collagen	COL1A1	NM_000088.3	Hs01076777_m1
α_1 chain type V collagen	COL5A1	NM_000093.3	Hs00609088_m1
baculoviral IAP repeat containing 5	BIRC5	NM_001012271.1	Hs03043575_m1
cyclin B1	CCNB1	NM_031966.3	Hs01030097_m1
cytidine 5'-triphosphate synthase	CTPS	NM_016748.2	Hs01041858_m1
elastin	ELN	NM_000501.2	Hs00355783_m1
lipoma HMGIC fusion partner-like 2	LHFPL2	NM_005779.2	Hs00299613_m1
lysyl oxidase	LOX	NM_002317.5	Hs00184700_m1
matrix metallopeptidase 14	MMP14	NM_004995.2	Hs01037009_g1
regulator of calcineurin 1	RCAN1	NM_004414.5	Hs01120954_m1
tenascin C	TNC	NM_002160.3	Hs01115665_m1
thrombospondin 2	THBS2	NM_003247.2	Hs01568063_m1
Wnt-1 inducible signaling pathway protein	WISP1	NM_003882.3	Hs00365573_m1

In vitro *TGFβ$_1$-stimulated myofibroblast differentiation.*

mRNA expression of genes highly correlated with new collagen formation was measured after TGFβ$_1$-stimulated myofibroblast differentiation. In short, normal human lung fibroblasts (NHLF) were obtained from Lonza Walkersville, Inc. (Walkersville, MD, USA) and cultured in Dulbecco's minimal essential medium (D-MEM; Invitrogen, Paisley, UK) supplemented with 10% fetal clone serum (FCS; HyClone, South Logan, UT, USA) and 1% antibiotic-antimycotic solution (100 U/ml penicillin, 100 µg/ml streptomycin, and 250 ng/ml amphotericin B (PSA), Sigma-Aldrich, St. Louis, MO, USA) in an incubator set at 37 °C, 95% humidity, and 5% CO_2. Cells from passage 6 were seeded in D-MEM with 10% FCS and 1% PSA at a density of 50,000 cells/cm^2 in a 24 wells plate. After allowing the cells to attach for 24 h, medium was replaced by D-MEM with 1% FCS and 1% PSA and 24 h later myofibroblast differentiation was induced by replacing the medium with D-MEM supplemented with 1%

FCS and 1% PSA containing 0 to 20 ng/ml recombinant human TGFβ_1 (PeproTech EC, London, UK). Fibroblasts were cultured for 24 or 48 h in the presence or absence of TGFβ_1 and mRNA samples were collected. mRNA was isolated using an RNeasy Mini Kit for RNA extraction (Qiagen, Hilden, Germany). The mRNA concentration was measured using a Nanodrop spectrophotometer (NanoDrop Technologies; Thermo-Fischer Scientific, Wilmington, DE, USA). mRNA was reverse-transcribed to complementary DNA (cDNA) using a High Capacity RNA-to-cDNA Kit (Applied Biosystems, Foster City, CA, USA). mRNA expression of ACTA2, COL1A1, ELN, WISP1, RCAN1, LHFPL2, TNC, MMP14, CTPS, LOX, THBS2, COL5A1, BIRC5, and CCNB1 and the housekeeping gene GAPDH was analyzed by Real-Time PCR performed on a 7500 Fast Real-Time PCR system (Applied Biosystems). GAPDH mRNA expression was determined using TaqMan® Rodent GAPDH Control Reagents (Applied Biosystems). All other genes were analyzed using unique TaqMan® Assays-on-Demand™ Gene Expression kits (Table 1; Applied Biosystems) specific for human.

Statistics

Statistical analyses were performed using SPSS (version 20, IBM Corporation, Armonk, NY, USA). Differences between animal groups were evaluated using one-way ANOVA with Dunnett's multiple comparisons test as a posthoc test to determine which groups were significant from the control group. Differences in gene expression in the *in vitro* studies were evaluated using two-way ANOVA with Bonferroni-adjusted t-tests as posthoc test to determine the effect of TGFβ_1.

Using Microsoft Office Excel (2007, Microsoft Corporation, Redmond, WA, USA) Pearson's correlation coefficient was calculated over all data points of all time points to correlate new collagen formation to single gene data, to scores for GO gene groups, and, in a separate experiment, to cell proliferation as measured by deuterated water incorporation in DNA.

Results

Fibrosis induction

Light microscopic analysis and the use of the modified Ashcroft fibrosis score (Figure 1) showed that fibrosis was strongly induced between week 0 and week 1, and remained high for at least 5 weeks after fibrosis induction by bleomycin.

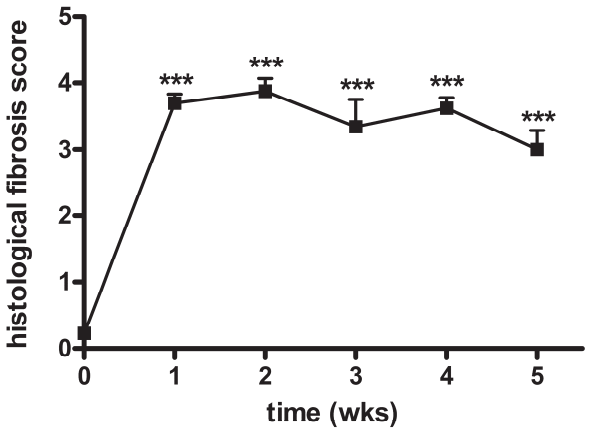

Figure 1: Fibrosis induction in mice treated with bleomycin.

Histological fibrosis score was determined from Masson's trichrome stained paraffin sections collected at 1 (n = 8), 2 (n = 8), 3 (n = 8), 4 (n = 6), and 5 (n = 7) weeks after intratracheal bleomycin instillation or from untreated animals at time point 0 (n = 7) as control. Results are given as mean ± SEM. *** $p < 0.001$.

New collagen formation

New collagen, determined as incorporation of deuterated water in Hyp, was significantly increased (9.3%, $p < 0.001$) one week after bleomycin administration in comparison to the level in control mice (1.1%) (Figure 2). The maximal formation of collagen was found two weeks after the bleomycin administration, when 10.1% ($p < 0.001$) of the collagen contained labelled Hyp. After this period the collagen deposition decreased steadily, leading eventually to 2.4% new collagen five weeks after bleomycin exposure, which is similar to control non-bleomycin treated mice (t=0). These data indicate that new collagen is mainly formed within the first weeks after bleomycin exposure.

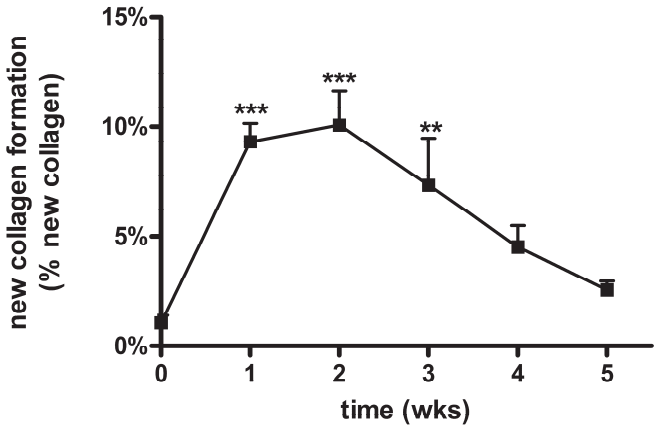

Figure 2: Kinetics of new collagen formation during bleomycin-induced lung fibrosis in mice.
Percentage of Hyp containing deuterated water as a measure of collagen deposited in the last 7 days before sacrifice at 1 (n = 8), 2 (n = 8), 3 (n = 8), 4 (n = 6), and 5 (n = 7) weeks after intratracheal bleomycin instillation or from untreated animals at time point 0 (n = 7) as control. Results are given as mean ± SEM. ** $p < 0.01$, *** $p < 0.001$.

Correlation between new collagen formation and gene expression

To study which processes are involved in collagen deposition in bleomycin-induced lung fibrosis, we correlated gene expression data from microarray analysis with the level of newly synthesized collagen in the individual animals. The genes that are most highly positively or negatively correlated with the deposition of collagen are shown in Table 2 and Table 3.

Extracellular matrix-related proteins were well represented in the group of genes highly positively correlated with collagen deposition. In this group there are extracellular matrix proteins such as elastin (r = 0.88), tenascin C (r = 0.85), and type V collagen (r = 0.81), but also proteins related to the collagen deposition machinery, such as thrombospondin 2 (r = 0.83), playing a role in fibril formation and lysyl oxidase (r = 0.84), important for the crosslinking of collagen. Furthermore, the collagen degrading enzyme MMP14 (r = 0.84) was positively correlated with collagen deposition.

Besides genes clearly related to extracellular matrix remodelling, collagen deposition also highly correlated with some genes not thought to be directly involved in extracellular matrix remodelling (Table 2), such as Wisp1. In the group of genes which showed a high negative correlation to collagen deposition, four genes encoding for ion channels were found: Slc7a4, Atp6v1c2, Atp2a2, and Atp2a3.

Table 2: Genes strongly positively correlated with new collagen formation.

Probe ID	Gene Symbol	Entrez Gene ID	Correlation to collagen deposition
6960079	Eln	13717	0.88
130239	Wisp1	22402	0.85
3440615	Rcan1	54720	0.85
6200397	Lhfpl2	218454	0.85
270324	Tnc	21923	0.85
3520066	Mmp14	17387	0.84
3140220	Ctps	51797	0.84
5420333	Tnc	21923	0.84
1410543	Lox	16948	0.84
6180678	Gusb	110006	0.83
2450347	Serpina3n	20716	0.83
6180168	Thbs2	21826	0.83
7050538	Ccl9	20308	0.82
780475	Prc1	233406	0.82
3710403	P2ry6	233571	0.82
5550201	Kdelr3	105785	0.82
580332	C1qb	12260	0.81
4150386	Col5a1	12831	0.81
150019	Litaf	56722	0.81
5810538	Ccdc80	67896	0.81
1470553	Cpxm1	56264	0.81
3710170	C1qc	12262	0.81
3830678	Fcgr3	14131	0.81
1240446	Birc5	11799	0.81
7550156	Ccnb1	268697	0.81
7200519	Cenpa	12615	0.80
50609	Hn1l	52009	0.80
6560341	Cd68	12514	0.80

Expression data of the set of expressed probes (resulting from microarray analysis) were mouse-per-mouse correlated with new collagen formation, using Pearson's correlation coefficient. Genes with a correlation >= 0.80 are shown.

Table 3: Genes strongly negatively correlated with new collagen formation.

Probe ID	Gene Symbol	Entrez Gene ID	Correlation to collagen deposition
3780193	Gsta3	14859	-0.85
2480730	Snhg11	319317	-0.84
3190646	Aox3	71724	-0.84
1470154	Mb	17189	-0.84
3520328	Glb1l2	244757	-0.84
2490672	Cbr2	12409	-0.83
940538	Slc7a4	224022	-0.83
830598	Cbx7	52609	-0.83
510093	Sfxn4	94281	-0.83
6940762	Atp6v1c2	68775	-0.82
770349	Atp2a2	11938	-0.82
4890112	Tppp3	67971	-0.81
7100731	Scgb3a2	117158	-0.81
60288	Atp2a3	53313	-0.81
1820286	Fmo3	14262	-0.81
430427	Ckmt2	76722	-0.80
6060086	Phactr1	218194	-0.80
6040689	Cyp2f2	13107	-0.80

Expression data of the set of expressed probes (resulting from microarray analysis) were mouse-per-mouse correlated with new collagen formation, using Pearson's correlation coefficient. Genes with a correlation <= -0.80 are shown.

Gene expression of correlated genes after in vitro *TGFβ$_1$-induced myofibroblast differentiation.*

Differentiation of normal human lung fibroblasts (NHLFs) to myofibroblasts by TGFβ$_1$-stimulation increased gene expression of the established fibrosis markers α-smooth muscle actin (αSMA; ACTA2, Figure 3A) and type I collagen (COL1A1, Figure 3B) after 24 and 48 h. Of the genes positively correlated with new collagen formation in bleomycin-induced lung fibrosis (Table 1), mRNA expression was upregulated by TGFβ$_1$-stimulation in the case of elastin (ELN, Figure 3C), Wnt-1 inducible signalling pathway protein 1 (WISP1, Figure 3D), tenascin C (TNC, Figure 3G), cytidine 5'-triphosphate synthase (CTPS, Figure 3I), lysyl oxidase (LOX, Figure 3J), thrombospondin 2 (THBS2, Figure 3K), type V collagen (COL5A1, Figure 3L), baculoviral IAP repeat containing 5 (BIRC5, Figure 3M), and cyclin B1 (CCNB1, Figure 3N). mRNA expression of lipoma HMGIC fusion partner-like 2 (LHFPL2, Figure 3F) and matrix metallopeptidase 14 (MMP14, Figure 3H) was not regulated by TGFβ$_1$ in NHLFs. For the regulator of calcineurin 1 (RCAN1) a significant interaction effect was found, indicating that the time influences the response of NHLFs to TGFβ$_1$ as clearly visible in Figure 3E.

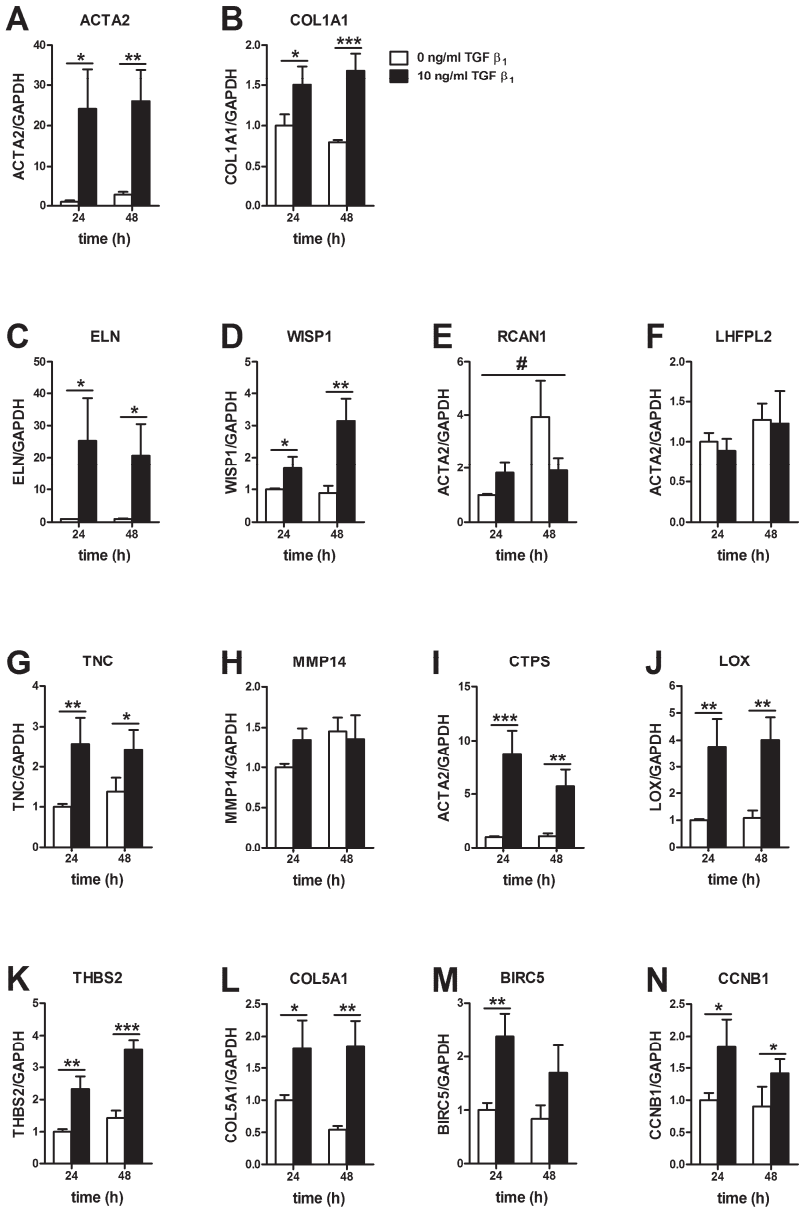

Figure 3: Genes correlated with new collagen formation are also upregulated in TGFβ$_1$-stimulated human lung fibroblasts.

Normal human lung fibroblasts were stimulated with 0 or 10 ng/ml TGFβ$_1$ for 24 or 48 h. Results are normalized for 0 ng/ml TGFβ$_1$ at 24 h and given as mean ± SD (n = 3 for control, n = 6 for TGFβ$_1$ stimulated cells). * $p < 0.05$, ** $p < 0.01$, *** $p < 0.001$, # significant interaction effect for time and TGFβ$_1$ stimulation ($p = 0.0005$).

Functional grouping of genes

Pathway enrichment analysis was performed to determine which pathways are overrepresented in the group of genes that are highly correlated with collagen deposition, using the Metacore pathway analysis tool. As input, we selected genes with a correlation coefficient higher than |0.75|, resulting in 142 positively and 68 negatively correlated genes. As expected, the pathway that was most represented in this group of genes was 'Cell adhesion - ECM remodelling' (Table 4). In addition, 'Cell Cycle' processes were prominently represented, which could indicate that cell proliferation is an important process contributing to collagen deposition during fibrosis development.

Table 4: Metacore pathways highly represented in genes correlated with new collagen formation.

Top Metacore pathways with correlated genes
Cell adhesion - ECM remodeling
Cell cycle - The metaphase checkpoint
Cell cycle - Role of Nek in cell cycle regulation
Cell cycle - Role of APC in cell cycle regulation
Transport - Clathrin-coated vesicle cycle
Reproduction - Progesterone-mediated oocyte maturation
Immune response - Oncostatin M signaling via JAK-Stat in mouse cells
wtCFTR and delta508 traffic / Clathrin coated vesicles formation (norm and CF)
Immune response - Oncostatin M signaling via JAK-Stat in human cells
Cell adhesion - Integrin-mediated cell adhesion and migration
Cytoskeleton remodeling - Regulation of actin cytoskeleton by Rho GTPases
Cell cycle - Initiation of mitosis
Cell cycle - Transition and termination of DNA replication
Cell cycle - Role of SCF complex in cell cycle regulation
Cytoskeleton remodeling - Cytoskeleton remodeling

Genes with a correlation coefficient higher than |0.75| were used as input for Metacore analysis. ECM, extracellular matrix

Analysis with the Tox-profiler software results in enrichment scores for GO gene groups for individual mice. This allowed us to correlate gene group enrichment values to collagen deposition as well, resulting in the list of gene groups depicted in Table 5. Of the 18 gene groups with the highest Pearson's correlation coefficients (> 0.7), 12 were related to cell division, further suggesting a role for cell proliferation in collagen deposition in fibrosis.

Table 5: Gene Ontology (GO) Gene sets strongly positively correlated with new collagen formation.

GO gene set	Correlation to collagen deposition
cell division	0.77
extracellular matrix structural constituent	0.77
positive regulation of endocytosis	0.76
positive regulation of phagocytosis	0.76
cell cycle process	0.75
cell cycle	0.75
spindle	0.75
chromosome, pericentric region	0.74
regulation of endocytosis	0.74
heparin binding	0.72
mitosis	0.72
M phase	0.72
M phase of mitotic cell cycle	0.72
mitotic cell cycle	0.72
cell cycle phase	0.72
DNA replication initiation	0.71
chromosomal part	0.71
protease inhibitor activity	0.70

Enrichment scores for GO gene sets were calculated for each mouse using Tox-profiler software and values were correlated with new collagen formation.

Correlation between new collagen formation and cell proliferation

To validate the relationship between collagen deposition and cell division, we determined the hypothesized combined presence of cell proliferation and collagen deposition using the deuterated water in a separate experiment. In this experiment deuterated water incorporation into collagen and deoxyribose was determined at the two week time point after bleomycin induction to analyse collagen deposition as well as newly synthesized DNA, as a measure for cell proliferation. New collagen formation and cell proliferation measured in the same lung sample showed a significant correlation ($r = 0.93$, $p < 0.001$, Figure 4).

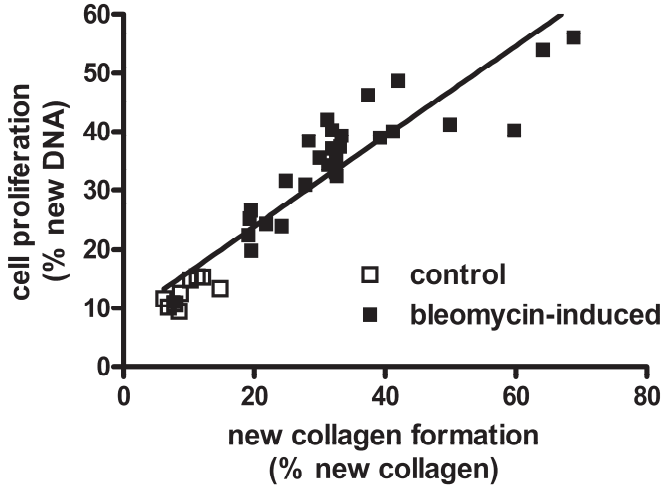

Figure 4: New collagen formation is correlated with cell proliferation, measured by deuterated water incorporation into DNA.

Mice received deuterated water for a period of two weeks before sacrifice and were sacrificed two weeks after bleomycin-instillation (closed squares) or PBS-instillation as control (open squares).

Discussion

The aims of this study were to investigate the dynamics of collagen formation during bleomycin-induced lung fibrosis and identify genes and processes correlated with core process of fibrosis: new collagen formation. To distinguish between newly formed collagen and collagen already present before the induction of experimental lung fibrosis, newly formed collagen was labelled using deuterated water. Correlation of new collagen formation data with gene expression revealed fibrosis-specific genes and processes.

New collagen formation analysis showed that collagen deposition had already strongly increased during the first week after bleomycin induction and decreased after three weeks to return to baseline levels after five weeks. The decrease in new collagen formation at the later time-points illustrates the transient nature of lung fibrosis induced by a single dose of bleomycin (Chua et al., 2005; Moeller et al., 2008). In a number of studies, it has been suggested that the main fibrotic phase during bleomycin-induced fibrosis only starts after the inflammatory phase in week 1 (Chaudhary et al., 2006; Moeller et al., 2008). Our data suggests that collagen deposition starts earlier than reported before and that collagen deposition and lung inflammation both occur during the early phase of bleomycin-induced lung fibrosis.

In response to bleomycin instillation into the lungs of mice, expression of a number of genes has been described to change (Brass et al., 2008; Kaminski et al., 2000). We could confirm the upregulation of osteopontin, tropoelastin, tenascin C, and heme-oxygenase, the four genes highest upregulated in the study of Kaminski and colleagues (Kaminski et al., 2000). However, a problem potentially encountered when using experimental models to elucidate disease-specific pathways is that it is difficult to differentiate between disease-specific pathways and model-specific pathways. For example, in our dataset an upregulation of genes related to apoptosis was found in week 1 (data not shown). This probably is the result of the reactive oxygen species produced by bleomycin. Although the resulting tissue damage strongly contributes to the development of fibrosis in this model, this does not necessarily mean that apoptosis is an important aspect of human lung fibrosis. To elucidate which processes are specifically related to the fibrotic process we measured both deposition of newly synthesized collagen and gene expression in each mouse in our study and correlated these parameters to obtain a gene expression signature of fibrosis within the lung: a list of genes and functional gene groups related to new collagen formation.

One interesting observation was the correlation between collagen deposition and cell proliferation-related gene groups in both our Metacore analysis and in the Gene Ontology (GO) Gene sets analysis performed using the Tox-profiler software. This was also demonstrated independently by the observation that cell proliferation and collagen synthesis, as measured by deuterated water incorporation, were significantly correlated. This suggests that cell proliferation is related to collagen deposition during bleomycin-

induced lung fibrosis in mice. Whether this is also the case in patients with IPF is unknown and has to be clarified. So far, only a few studies are published on this topic. It has been hypothesized that cellularity is an important predictor for prognosis of patients with IPF (Fulmer et al., 1979). Selman and colleagues (Zuo et al., 2002) compared microarray results from patients with IPF to those of patients suffering from hypersensitivity pneumonitis. Genes that were higher upregulated in IPF than in hypersensitivity pneumonitis could be categorized as involved in development, extracellular structure and turnover, and, interestingly, also cellular growth and differentiation, indicating that in the later phase of fibrosis cellular growth is important in IPF. However, to what extent increased cell proliferation is important in end stage human disease is unclear, since cellularity of lung biopsies was found not to be predictive for survival of IPF patients (King Jr. et al., 2001).

In addition to functional gene groups, we also correlated expression of single genes to collagen deposition. The gene most highly correlated with collagen deposition was elastin. Upregulation of elastin has been shown in a different model for lung fibrosis using butylated hydroxytoluene with 70% oxygen (Hoff et al., 1999). Furthermore, morphometric analysis of elastin fibres in histological samples have also shown an increase of elastin in human IPF patients (Cha et al., 2010), but to our knowledge our study is the first to show a clear correlation between collagen deposition and elastin gene expression.

The correlation between type I collagen gene expression and collagen protein deposition ($r = 0.62$) was not as high as for elastin. This might be related to the strong dependence of the actual amount of collagen formation on the many post-translational modifications involved in collagen synthesis, including presence and activity of chaperone proteins like hsp47, collagen modification enzymes, such as prolyl hydroxylases and lysyl hydroxylases, and enzymes involved in collagen modification like lysyl oxidases. Interestingly, several of these genes highly correlate with new collagen formation. For example, thrombospondin 2, playing a role in fibril formation, and lysyl oxidase, important for the crosslinking of collagen were highly correlated.

In addition to elastin, other extracellular matrix proteins correlating to new collagen formation were tenascin C and type V collagen. Furthermore, other genes, not directly related to collagen deposition, could be identified (see Table 1). One example is the Wisp1 gene, encoding for 'Wnt-1 inducible signalling pathway protein 1'. Wisp1 is upregulated in IPF (Konigshoff et al., 2009) and systemic sclerosis (Lemaire et al., 2010), while neutralizing antibodies for Wisp1 reduced bleomycin-induced lung fibrosis (Konigshoff et al., 2009). Furthermore, Wnt signalling is upregulated in systemic scleroderma patients (Lemaire et al., 2010; Wei et al., 2012), wound healing (Cheon et al., 2002) and aging-associated muscle fibrosis (Brack et al., 2007). More recently, expression of survivin, encoded by 'Birc5', was shown to be upregulated in IPF fibroblasts, compared to lung fibroblasts from healthy controls (Sisson et al., 2012). These authors also report increased survivin expression in response to $TGF\beta_1$ stimulation. Also one of the genes negatively correlated with collagen

deposition, Scgb3a2, has been described recently to have a role in pulmonary fibrosis (Kurotani et al., 2011). This gene encodes for member 2 of family 3A of the secretoglobins, and was related to a suppression of TGFβ-signalling resulting in less fibrosis in response to bleomycin. These three examples of genes described to be related to bleomycin-induced fibrosis, indicate that with our approach of correlating gene expression to collagen deposition it is possible to identify these fibrosis-relevant genes. This implies that the genes highly correlated with collagen deposition in our model are interesting targets for mechanistic understanding and therapeutic possibilities for pulmonary fibrosis.

Among the negatively correlated genes, four genes encoding for ion channels were present. Since ion channels are relatively abundant in epithelial cells, this suggests that epithelial cell damage, resulting in a reduction of ion channel gene expression, is related to fibrosis-related new collagen formation. This confirms that epithelial cell damage is important in fibrosis, as has been proposed in the literature (Selman and Pardo, 2002).

In our microarray we analyzed gene expression from total lung lysates. As a result, we do not know which cell type is responsible for upregulation of a specific gene during bleomycin-induced lung fibrosis. Therefore, we investigated a possible role for lung fibroblasts in the increased gene expression *in vitro* in human lung fibroblasts. We simulated the fibrotic environment of fibroblasts by addition of $TGF\beta_1$. Of the 12 genes that were positively correlated with new collagen formation in bleomycin-induced lung fibrosis and were analyzed in this model, 9 were upregulated by $TGF\beta_1$. Thus, lung fibroblasts under fibrotic conditions express higher levels of these genes, which confirms a possible role for fibroblasts in the upregulation of these genes in the *in vivo* model. Furthermore, the fact that in the *in vitro* experiments human fibroblasts increased expression of these genes, indicates that our results from the *in vivo* mouse model are relevant for human pulmonary fibrosis.

In conclusion, our data indicate that determining collagen deposition by labelling with deuterated water gives more detailed information about collagen deposition in a defined time period during the development of lung fibrosis. We constructed a gene expression signature of fibrosis within the lung and identified genes and pathways related to collagen deposition during bleomycin-induced lung fibrosis by combining new collagen formation data with gene expression data. These data demonstrate that the core process of fibrosis, i.e. the formation of new collagen, correlates not only with a wide range of genes involved in general extracellular matrix production and modification but also with cell proliferation. In addition, we identified other genes not directly involved in extracellular matrix production that strongly correlated with new collagen formation. Upregulation after *in vitro* $TGF\beta_1$-induced myofibroblast differentiation provided further evidence for the involvement of these correlating genes in the process of lung fibrosis, possibly leading us to future therapeutic options for this devastating lung disease.

Acknowledgements

The authors would like to thank Joline Attema and Jessica Snabel for the technical assistance and André Boorsma for the useful discussion.

References

Boorsma, A., Foat, B.C., Vis, D., Klis, F., Bussemaker, H.J., 2005. T-profiler: scoring the activity of predefined groups of genes using gene expression data. Nucleic Acids Res. 33, W592–W595.

Brack, A.S., Conboy, M.J., Roy, S., Lee, M., Kuo, C.J., Keller, C., Rando, T.A., 2007. Increased Wnt signaling during aging alters muscle stem cell fate and increases fibrosis. Science 317, 807–10.

Brass, D.M., Yang, I. V, Kennedy, M.P., Whitehead, G.S., Rutledge, H., Burch, L.H., Schwartz, D.A., 2008. Fibroproliferation in LPS-induced airway remodeling and bleomycin-induced fibrosis share common patterns of gene expression. Immunogenetics 60, 353–369.

Cha, S.I., Groshong, S.D., Frankel, S.K., Edelman, B.L., Cosgrove, G.P., Terry-Powers, J.L., Remigio, L.K., Curran-Everett, D., Brown, K.K., Cool, C.D., Riches, D.W., 2010. Compartmentalized expression of c-FLIP in lung tissues of patients with idiopathic pulmonary fibrosis. Am. J. Respir. Cell Mol. Biol. 42, 140–148.

Chaudhary, N.I., Schnapp, A., Park, J.E., 2006. Pharmacologic differentiation of inflammation and fibrosis in the rat bleomycin model. Am. J. Respir. Crit. Care Med. 173, 769–776.

Cheon, S.S., Cheah, A.Y.L., Turley, S., Nadesan, P., Poon, R., Clevers, H., Alman, B.A., 2002. beta-Catenin stabilization dysregulates mesenchymal cell proliferation, motility, and invasiveness and causes aggressive fibromatosis and hyperplastic cutaneous wounds. Proc. Natl. Acad. Sci. USA 99, 6973–8.

Chua, F., Gauldie, J., Laurent, G.J., 2005. Pulmonary fibrosis: searching for model answers. Am. J. Respir. Cell Mol. Biol. 33, 9–13.

Degryse, A.L., Tanjore, H., Xu, X.C., Polosukhin, V.V., Jones, B.R., Boomershine, C.S., Ortiz, C., Sherrill, T.P., McMahon, F.B., Gleaves, L.A., Blackwell, T.S., Lawson, W.E., 2011. TGFβ signaling in lung epithelium regulates bleomycin-induced alveolar injury and fibroblast recruitment. Am. J. Physiol. Lung Cell Mol. Physiol. 300, L887–97.

Edgar, R., Domrachev, M., Lash, A.E., 2002. Gene Expression Omnibus: NCBI gene expression and hybridization array data repository. Nucleic Acids Res. 30, 207–10.

Fernandez Perez, E.R., Daniels, C.E., Schroeder, D.R., St, S.J., Hartman, T.E., Bartholmai, B.J., Yi, E.S., Ryu, J.H., 2010. Incidence, prevalence, and clinical course of idiopathic pulmonary fibrosis: a population-based study. Chest 137, 129–137.

Fulmer, J.D., Roberts, W.C., Von Gal, E.R., Crystal, R.G., 1979. Morphologic-physiologic correlates of the severity of fibrosis and degree of cellularity in idiopathic pulmonary fibrosis. J. Clin. Invest 63, 665–676.

Gaeng, D.P., Geiser, M., Cruz-Orive, L.M., Larsen, S.E., Schaffner, T., Laissue, J.A., Altermatt, H.J., 1995. Paradoxical effects of bleomycin and heavy water (D2O) in mice. Int. J. Cancer 62, 784–90.

Gardner, J.L., Turner, S.M., Bautista, A., Lindwall, G., Awada, M., Hellerstein, M.K., 2007. Measurement of liver collagen synthesis by heavy water labeling: effects of profibrotic toxicants and antifibrotic interventions. Am. J. Physiol. Gastrointest. Liver Physiol. 292, G1695–705.

Hannivoort, R.A., Hernandez-Gea, V., Friedman, S.L., 2012. Genomics and proteomics in liver fibrosis and cirrhosis. Fibrogenesis Tissue Repair 5, 1.

Hoff, C.R., Perkins, D.R., Davidson, J.M., 1999. Elastin gene expression is upregulated during pulmonary fibrosis. Connect. Tissue Res. 40, 145–53.

Hübner, R.-H., Gitter, W., El Mokhtari, N.E., Mathiak, M., Both, M., Bolte, H., Freitag-Wolf, S., Bewig, B., 2008. Standardized quantification of pulmonary fibrosis in histological samples. Biotechniques 44, 507–517.

Kaminski, N., Allard, J.D., Pittet, J.F., Zuo, F., Griffiths, M.J., Morris, D., Huang, X., Sheppard, D., Heller, R.A., 2000. Global analysis of gene expression in pulmonary fibrosis reveals distinct programs regulating lung inflammation and fibrosis. Proc. Natl. Acad. Sci. USA 97, 1778–1783.

King Jr., T.E., Schwarz, M.I., Brown, K., Tooze, J.A., Colby, T. V, Waldron Jr., J.A., Flint, A., Thurlbeck, W., Cherniack, R.M., 2001. Idiopathic pulmonary fibrosis: relationship between histopathologic features and mortality. Am. J. Respir. Crit. Care Med. 164, 1025–1032.

Konigshoff, M., Kramer, M., Balsara, N., Wilhelm, J., Amarie, O. V, Jahn, A., Rose, F., Fink, L., Seeger, W., Schaefer, L., Gunther, A., Eickelberg, O., 2009. WNT1-inducible signaling protein-1 mediates pulmonary fibrosis in mice and is upregulated in humans with idiopathic pulmonary fibrosis. J. Clin. Invest. 119, 772–787.

Kurotani, R., Okumura, S., Matsubara, T., Yokoyama, U., Buckley, J.R., Tomita, T., Kezuka, K., Nagano, T., Esposito, D., Taylor, T.E., Gillette, W.K., Ishikawa, Y., Abe, H., Ward, J.M., Kimura, S., 2011. Secretoglobin 3A2 suppresses bleomycin-induced pulmonary fibrosis by transforming growth factor beta signaling down-regulation. J.Biol.Chem. 286, 19682–19692.

Lemaire, R., Farina, G., Bayle, J., Dimarzio, M., Pendergrass, S.A., Milano, A., Perbal, B., Whitfield, M.L., Lafyatis, R., 2010. Antagonistic effect of the matricellular signaling protein CCN3 on TGF-beta- and Wnt-mediated fibrillinogenesis in systemic sclerosis and Marfan syndrome. J. Invest. Dermatol. 130, 1514–23.

Moeller, A., Ask, K., Warburton, D., Gauldie, J., Kolb, M., 2008. The bleomycin animal model: a useful tool to investigate treatment options for idiopathic pulmonary fibrosis? Int. J. Biochem. Cell Biol. 40, 362–382.

Neese, R.A., Misell, L.M., Turner, S., Chu, A., Kim, J., Cesar, D., Hoh, R., Antelo, F., Strawford, A., McCune, J.M., Christiansen, M., Hellerstein, M.K., 2002. Measurement in vivo of proliferation rates of slow turnover cells by 2H2O labeling of the deoxyribose moiety of DNA. Proc. Natl. Acad. Sci. USA 99, 15345–15350.

Neese, R.A., Siler, S.Q., Cesar, D., Antelo, F., Lee, D., Misell, L., Patel, K., Tehrani, S., Shah, P., Hellerstein, M.K., 2001. Advances in the stable isotope-mass spectrometric measurement of DNA synthesis and cell proliferation. Anal. Biochem. 298, 189–195.

Previs, S.F., Hazey, J.W., Diraison, F., Beylot, M., David, F., Brunengraber, H., 1996. Assay of the deuterium enrichment of water via acetylene. J. Mass Spectrom. 31, 639–642.

Selman, M., Pardo, A., 2002. Idiopathic pulmonary fibrosis: an epithelial/fibroblastic cross-talk disorder. Respir. Res. 3, 3–8.

Sisson, T.H., Maher, T.M., Ajayi, I.O., King, J.E., Higgins, P.D.R., Booth, A.J., Sagana, R.L., Huang, S.K., White, E.S., Moore, B.B., Horowitz, J.C., 2012. Increased survivin expression contributes to apoptosis-resistance in IPF fibroblasts. Adv. Biosci. Biotechnol. 3, 657–664.

Tanjore, H., Xu, X.C., Polosukhin, V. V, Degryse, A.L., Li, B., Han, W., Sherrill, T.P., Plieth, D., Neilson, E.G., Blackwell, T.S., Lawson, W.E., 2009. Contribution of epithelial-derived fibroblasts to bleomycin-induced lung fibrosis. Am. J. Respir. Crit. Care Med. 180, 657–665.

Varady, K.A., Roohk, D.J., Hellerstein, M.K., 2007. Dose effects of modified alternate-day fasting regimens on in vivo cell proliferation and plasma insulin-like growth factor-1 in mice. J. Appl. Physiol 103, 547–551.

Wei, J., Fang, F., Lam, A.P., Sargent, J.L., Hamburg, E., Hinchcliff, M.E., Gottardi, C.J., Atit, R., Whitfield, M.L., Varga, J., 2012. Wnt/β-catenin signaling is hyperactivated in systemic sclerosis and induces Smad-dependent fibrotic responses in mesenchymal cells. Arthritis Rheum. 64, 2734–2745.

Zuo, F., Kaminski, N., Eugui, E., Allard, J., Yakhini, Z., Ben-Dor, A., Lollini, L., Morris, D., Kim, Y., DeLustro, B., Sheppard, D., Pardo, A., Selman, M., Heller, R.A., 2002. Gene expression analysis reveals matrilysin as a key regulator of pulmonary fibrosis in mice and humans. Proc. Natl. Acad. Sci. USA 99, 6292–6297.